Targeted Delivery of Doxorubicin via Sterically Stabilized Immunoliposomes: Pharmacokinetics and Biodistribution in Tumor-bearing Mice[1]

Noam Emanuel,[2,5] Eli Kedar,[2] Elijah M. Bolotin,[3] Nechama I. Smorodinsky,[4] and Yechezkel Barenholz[3,6]

Received January 31, 1996; accepted March 21, 1996

Purpose. To evaluate benefits in tumor localization, availability, and noncancerous organ distribution of doxorubicin (DOX) delivered via small (≤120 nm) sterically stabilized immunoliposomes targeted against a tumor-associated antigen in fibrosarcoma-bearing mice.

Methods. DOX-loaded liposomes were prepared with (i) specific monoclonal IgG_3 antibody (32/2, D-SSIL-32/2); (ii) non-specific IgG_3 (D-SSIL-IgG); or (iii) no IgG (D-SSL) on their surface. Equal DOX amounts were injected intravenously via each type of liposome into BALB/c mice carrying experimental lung metastases of a polyoma virus-induced fibrosarcoma (A9 ctc 220) expressing a polyoma virus-induced tumor-associated antigen (PAA) on their surface. Metastases occurred mainly in lung. Mice were treated at 3 stages of tumor development (micrometastases, medium-size metastases, and large, necrotic metastases). Performance evaluation was based on time-dependent quantification of DOX and DOX metabolites (DOX-M) in lung tumor, noncancerous organs, and plasma.

Results. (i) DOX delivered via both SSIL retained the prolonged circulation time typical of DOX delivered via D-SSL. (ii) DOX accumulation in noncancerous organs was similar for all preparations. Low levels of DOX-M were obtained for all three preparations in all organs except liver, suggesting a similar processing. (iii) Preparations differed in behavior in lung tumor depending on tumor size and microanatomy. Only at the micrometastases stage were the specifically targeted D-SSIL-32/2 superior to D-SSL and D-SSIL-IgG, delivering 2–4 times more drug into the tumor. (iv) DOX-M level in all three tumor stages was in the following order: D-SSIL-32/2 >> D-SSL >> D-SSIL-IgG, suggesting that DOX delivered as D-SSIL-32/2 is most available to tumor cells.

Conclusions. The advantage of specific targeting of sterically stabilized liposomes is expressed mainly in increasing availability of DOX to tumor cells in a way which is dependent on tumor microanatomy. The impact of this advantage to therapeutic efficacy remains to be determined.

KEY WORDS: sterically stabilized immunoliposomes; targeting; doxorubicin; lung metastases; pharmacokinetics; biodistribution.

INTRODUCTION

Doxorubicin (DOX)-loaded sterically stabilized liposomes (SSL) of ~100 nm deliver much higher levels of drug to tumors in animals (1) and humans (1,2) than are obtained with the free drug. However, accumulation of DOX-loaded SSL (D-SSL) in solid tumors is rather slow; for example, DOX peak levels in human tumors occur 3–6 days after D-SSL administration (2). D-SSL performance might be improved by active targeting, using a ligand on its surface which recognizes the tumor cells, thereby facilitating binding of the liposomes and subsequent drug uptake by the tumor cells. These liposomes are referred to as ligandoliposomes, and when the ligands are antibodies, as immunoliposomes. With systemically administered antibody-coated conventional liposomes, targeting to most solid tumors was not feasible, due mainly to the rapid uptake of the liposomes by the reticuloendothelial system (RES) (3,4). This obstacle to liposome targeting may be overcome by using small (<120 nm) SSL since their integrity in serum is maintained and RES uptake is dramatically reduced (1,5).

Sterically stabilized immunoliposomes (SSIL) prepared in various ways (6–9), retaining both immunospecificity and steric stabilization, can be targeted to intravascular components (7,8). Moreover, in at least one tumor model in mice it was demonstrated that D-SSIL are more efficacious than D-SSL in treating small metastatic solid tumors (10).

This study is aimed at evaluating three steps in comparative evaluation of D-SSL and D-SSIL in tumor-bearing mice: (i) plasma, organ, and tumor pharmacokinetics of encapsulated DOX; (ii) drug availability to cells as assessed from rate and extent of DOX metabolism in noncancerous and cancerous tissues; and (iii) effect of tumor size and microanatomy on (ii).

MATERIALS AND METHODS

Reagents for Liposome Preparation

Sources, preparation and characterization of reagents, including lipids and antibodies, were as previously reported (9,11).

Cell Lines

A9 ctc 220 tumor cells (referred to as A9 cells) that were used as the specific target for binding IgG_3 mouse MAb NI32/2/4 (32/2) are similar to those described by Emanuel et al. (9) except that this tumor subline has a lower metastatic capacity and a lower density of PAA on its surface.

[1] This work was supported by grants from the Israel Cancer Association and the Israel Cancer Research Fund to E. Kedar and Y. Barenholz.

[2] The Lautenberg Center for General and Tumor Immunology, The Hebrew University-Hadassah Medical School, Jerusalem 91120, Israel.

[3] Department of Biochemistry, The Hebrew University-Hadassah Medical School, Jerusalem 91120, Israel.

[4] Department of Cell Research and Immunology, George S. Wise Faculty of Life Sciences, Tel Aviv University, Tel Aviv 69978, Israel.

[5] To whom requests for reprints should be addressed.

[6] To whom correspondence should be addressed.

ABBREVIATIONS: AUC, area under the curve; D-Lip, doxorubicin-loaded Lip; DOL, doxorubicinol; DOX, doxorubicin; DOX-M, doxorubicin metabolites; D-SSIL, doxorubicin-loaded SSIL; D-SSL, doxorubicin-loaded SSL; FITC-PE, fluorescein isothiocyanate-phosphatidylethanolamine; HPLC, high performance liquid chromatography; ID, injected dose; IgG, immunoglobulin G; Lip, nonstabilized liposomes; MAb, monoclonal antibodies; MRT, mean residence time; PAA, polyoma virus-induced tumor-associated antigen; PEG, polyethylene glycol; PEG-DSPE, *N*-carbamyl-poly-(ethylene glycol methyl ether)-1,2-distearoyl-*sn*-glycero-3-phosphoethanolamine triethyl ammonium salt; RES, reticuloendothelial system; SSIL, sterically stabilized immunoliposomes; SSIL-IgG, normal mouse IgG conjugated to SSL; SSIL-32/2, 32/2 MAb conjugated to SSL; SSL, sterically stabilized liposomes; 7d-DOLON, 7-deoxydoxorubicinol-one; 7d-DOXON, 7-deoxydoxorubicinone; 32/2, NI32/2/4 MAb.

0724-8741/96/0600-0861$09.50/0

Animals

Specific pathogen-free BALB/c female mice, aged 9–12 weeks, were obtained from Harlan Sprague Dawley (Indianapolis, IN). Groups consisted of 4–6 mice for each time point.

Tumor Model

BALB/c mice were inoculated iv with 5×10^5 A9 cells to obtain experimental metastases. These cells settled and metastasized only in the lungs. Three different tumor stages as defined by size of lung metastases were studied: Stage I—micrometastases (tumor weight $\leq$ 0.01 g), Stage II—medium-size metastases (0.05–0.1 g), Stage III—large, necrotic metastases ($\geq$ 0.8 g), occurring 14, 20, and 26 days post tumor inoculation, respectively. Without treatment, most mice died of lung tumors 35–45 days post inoculation.

Preparation of Sterically Stabilized Liposomes (SSL) and Immunoliposomes (SSIL)

SSL and SSIL loaded with DOX (D-SSL and D-SSIL, respectively) or fluorescently labeled with FITC-PE were prepared and characterized as described elsewhere (9,11,12). In some experiments, conventional liposomes (Lip) were also used.

Pharmacokinetic and Biodistribution Studies in Tumor-Bearing Mice

The plasma pharmacokinetics included studies of the time-dependent clearance of: (i) liposomes without DOX, using 0.1 mole % FITC-PE-labeled SSIL, SSL, and Lip; and (ii) DOX delivered as free drug and as D-SSIL-32/2, D-SSIL-IgG, D-SSL, and D-Lip. All liposomes and free DOX were diluted in sterile pyrogen-free 10% sucrose solution and injected (0.2 ml) into the tail veins of ~20-g mice. For the DOX-containing liposomes, each mouse received 35 μg DOX and ~0.35 μmoles phospholipids.

At the desired time, blood (0.5 ml) was collected from the retroorbital sinus after ether anesthesia into test tubes containing K_3-EDTA as anticoagulant, and plasma was separated by centrifugation. A similar hematocrit of ~50% was obtained for all blood samples. Mice were immediately sacrificed, and their organs removed, washed in cold phosphate-buffered saline, dried over filter paper, and weighed. Plasma and organs were either processed immediately as described below or kept frozen at −70°C until analysis.

Aliquots of plasma of mice injected with FITC-PE-labeled liposomes (SSIL-32/2, SSIL-IgG, and SSL) were diluted in alkaline (borate buffer) isopropanol pH 9.5 to the range in which fluorescence (excitation 495 nm, emission 525 nm) is proportional to FITC-PE concentration. A calibration curve in saline/isopropanol pH 9.5 was used to determine FITC-PE concentration in plasma.

Extraction of DOX and DOX metabolites (DOX-M) from plasma and organs was performed as described by Cummings and McArdle (13). DOX and DOX-M were analyzed by HPLC (2,9). Daunorubicin (retention time [RT], 8.00 min) was used as internal standard. Synthetically prepared doxorubicinol (DOL) (RT, 3.16 min), 7-deoxydoxorubicinol aglycone (7-deoxydoxorubicinol-one, 7d-DOLON) (RT, 1.95 min), and 7-deoxydoxorubicinone (7d-DOXON) (RT, 2.83 min) were used as markers. RT of DOX was 4.46 min (2). Recoveries were always >80% and could be corrected by using the internal standard. HPLC assay sensitivity limit was 0.5 ng per peak (equivalent to 6.25 ng/ml plasma [~0.018% of injected dose]).

The identification of DOX-M was confirmed by TLC analysis (2). Blood volume for mice was assumed to be 77.8 ml/kg body weight; tissue DOX and DOX-M concentrations were corrected for plasma volume (14).

Nonlinear least-squares analysis was performed on pharmacokinetic and biodistribution data using Rstrip software (Micromath, Salt Lake City) (2).

Statistical Evaluation

The significance of the data was evaluated using Student's *t*-test (two-tailed). P values < 0.05 were considered significant.

RESULTS

Plasma Pharmacokinetics

The two D-SSIL preparations used in these experiments behaved similarly in tumor-bearing mice irrespective of antibody specificity, but differed from the D-SSL to a larger extent than in normal mice with respect to DOX plasma pharmacokinetics (data for Stage II are shown in Fig. 1 and Table 1). While clearance of DOX delivered via D-SSL was nearly monophasic, it was clearly biphasic for DOX delivered via D-SSIL. Despite the initial fast clearance, >10% of the drug delivered via D-SSIL remained in the plasma 24 h post-injection.

Total DOX-M level in plasma was very low for all three liposome preparations (Fig. 1); however, the lowest level was obtained with D-SSL, plateauing at 1% of the injected dose (ID) 6 h post-injection, compared with 2–2.5% for the two D-SSIL preparations ($p < 0.05$).

To follow the plasma pharmacokinetics of the carrier itself without the drug, Lip, SSL, and SSIL were labeled with 0.1 mole % nontransferable liposome marker FITC-PE (9,11). The pharmacokinetics of FITC-PE-labeled liposomes in normal mice was found to be almost identical to that of DOX-loaded liposomes. For example, 24 h post-injection the level of FITC-D-Lip was reduced to <0.1% of the ID, while levels of FITC-labeled SSL and SSIL were >10% of the ID (data not shown).

Biodistribution of DOX and Its Metabolites in Tumor-Free Organs of Tumor-Bearing Mice

Time-dependent biodistribution of DOX and its total metabolites (DOX-M) was determined at 2, 6, and 24 h in the liver, spleen, kidney, and heart of mice injected iv with 35 μg DOX as D-SSL, D-SSIL-IgG, or D-SSIL-32/2. Organ distributions in tumor-bearing mice at tumor Stage I (micrometastases) and Stage II were almost identical. In all mice tested there was no effect of treatment on organ weight (see Fig. 2 legend). Only slight differences were found between the D-SSL, D-SSIL-IgG, and D-SSIL-32/2 regarding organ DOX levels, as demonstrated in Fig. 2 for mice with Stage II tumors. Only in spleen, the level of DOX delivered via the two D-SSIL preparations was 1.5–2.0 times higher at all time points than that delivered by D-SSL, but this did not result in greater accumulation of DOX-M. For the three liposomal preparations the ratio of DOX-M to DOX in the liver was 3–5 times higher than in all other organs tested. In heart, for all three

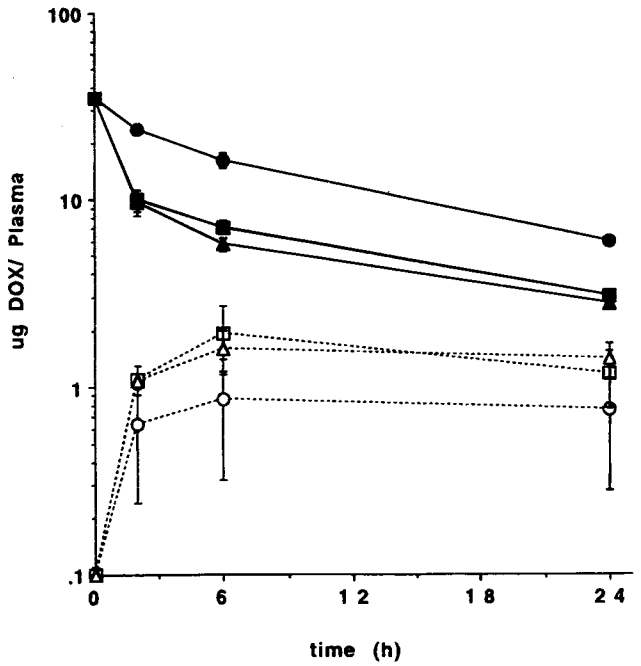

Fig. 1. Plasma pharmacokinetics of DOX encapsulated in liposomes and immunoliposomes in tumor-bearing mice. DOX (35 μg/mouse) was injected iv as D-SSL (●), D-SSIL-IgG (■), or D-SSIL-32/2 (▲). Plasma DOX levels were measured as a function of time in mice bearing A9 tumor lung metastases, Stage II (see text). Total DOX-M values (open symbols and dashed lines) were calculated as the sum of all metabolites. Results are given as μg DOX corrected for total mouse plasma volume (14). DOX and DOX-M were determined by HPLC (for more details see Materials and Methods). The values are means ± S.D. Statistical analysis (p values). For DOX: D-SSL vs. D-SSL-IgG and vs. D-SSIL-32/2 < 0.02 at all time points; D-SSIL-32/2 vs. D-SSIL-IgG > 0.05 at 2 h and 24 h, < 0.05 at 6 h. For DOX-M: D-SSL vs. D-SSL-IgG < 0.05 at 2 h and 6 h, > 0.05 at 24 h;D-SSL vs. D-SSIL-32/2 < 0.05 at all time points; D-SSIL-32/2 vs. D-SSIL-IgG > 0.05 at all time points.

Table 1. Plasma Pharmacokinetics of DOX After I.V. Injection of DOX-loaded Liposomes and Immunoliposomes in Normal and Tumor-bearing Mice[a]

Mice	Liposomes	Clearance (ml/h)	MRT (h)	AUC^{24} (μg/ml/h)	Vss[d] (ml)
Normal[b]	D-SSL	0.08	8.8	428	0.72
	D-SSIL-IgG	0.12	6.6	297	0.78
	D-Lip	0.44	1.8	80	0.77
Tumor-bearing[c]	D-SSL	0.09	7.4	369	0.70
	D-SSIL-IgG	0.33	2.6	112	0.82
	D-SSIL-32/2	0.35	2.4	101	0.81

[a] 35 μg DOX injected with each preparation.
[b] Normal BALB/c mice (data from ref. 9).
[c] BALB/c mice with Stage II lung metastases.
[d] Volume of distribution.

preparations, concentrations of DOX and DOX-M were below detectable levels.

Pharmacokinetics and Accumulation of DOX and Its Metabolites in Cancerous Lungs

The time-dependent accumulation of DOX (Fig. 3) and DOX-M (Fig. 4) in the lungs for the three tumor stages was compared at 2 and 6 h post-injection for D-SSL, D-SSIL-IgG, and D-SSIL-32/2. For DOX, the three liposomal preparations have similar pharmacokinetics in mice with Stage II tumor (Fig. 3B). At Stage I (Fig. 3A), the D-SSIL-32/2 has a significantly faster rate (at 2 h) of delivering drug than the other preparations ($p < 0.01$). In mice with large, necrotic tumors (Stage III, Fig. 3C), the two D-SSIL preparations behave similarly irrespective of the type of IgG attached, with drug reaching concentrations considerably lower than those reached in lungs with smaller tumors (Figs. 3A and 3B). The peak drug level in the tumor is in the order: Stage II > Stage I >> Stage III.

The superiority of D-SSIL-32/2 over D-SSIL-IgG for all tumor stages is more evident when DOX-M is measured rather than DOX itself (Fig. 4). While for the D-SSIL-IgG no metabolites were evident (Fig. 4), a similar concentration of DOX for both D-SSIL-IgG and D-SSIL-32/2 reached the tumorous lungs (Fig. 3). The highest ratio of DOX-M to DOX (~0.5) was achieved for the D-SSIL-32/2 in large tumors.

Figure 5 shows differences in profiles of several metabolites in the tumor (Stage II) at 2 and 6 h post-injection for D-SSL and D-SSIL-32/2. At 2 h, metabolites (mainly 7d-DOXON) were observed only after injection of D-SSIL-32/2. At 6 h, there was a higher level of metabolites, especially 7d-DOLON, in mice injected with D-SSIL-32/2 than in mice injected with D-SSL. There was no measurable 7d-DOLON in lungs of mice injected with D-SSL. There were no detectable levels of metabolites in mice given D-SSIL-IgG. For Stages I and III of the tumor, only 7d-DOXON was found for all liposome preparations (data not shown).

Tumor selectivity of the drug delivered via the three liposome preparations is described in Fig. 6, showing the ratio of the concentration of total drug (DOX + DOX-M) in plasma and organs of mice with Stage II tumors to that in normal mice. Significant selectivity was found only in the cancerous lung. D-SSIL-IgG had little or no selectivity, while D-SSL and D-SSIL-32/2 showed distinct tumor selectivity, that for D-SSIL-32/2 (ratio = 9.0) being significantly greater than that for D-SSL (ratio = 4.5).

Tumor selectivity of D-SSIL-32/2, relative to other liposome preparations, was confirmed in localization experiments in which frozen tissue sections were taken from tumorous lungs at the stage of micrometastases 2 h after iv injection. The fluorescence of DOX and its metabolites permits their localization. Lung sections taken from mice injected with D-SSIL-32/2 showed many more strongly fluorescent spots (indicating drug localization in the tumor mass itself) than those from mice injected with other liposome preparations. In the former, intense fluorescence was seen in the extravascular space, reaching 2–3 layers of tumor cells beyond the endothelial layer of the blood vessels (data not shown).

DISCUSSION

The uniqueness of this study is that special emphasis was placed on (a) analyzing the effect of tumor stage on liposome

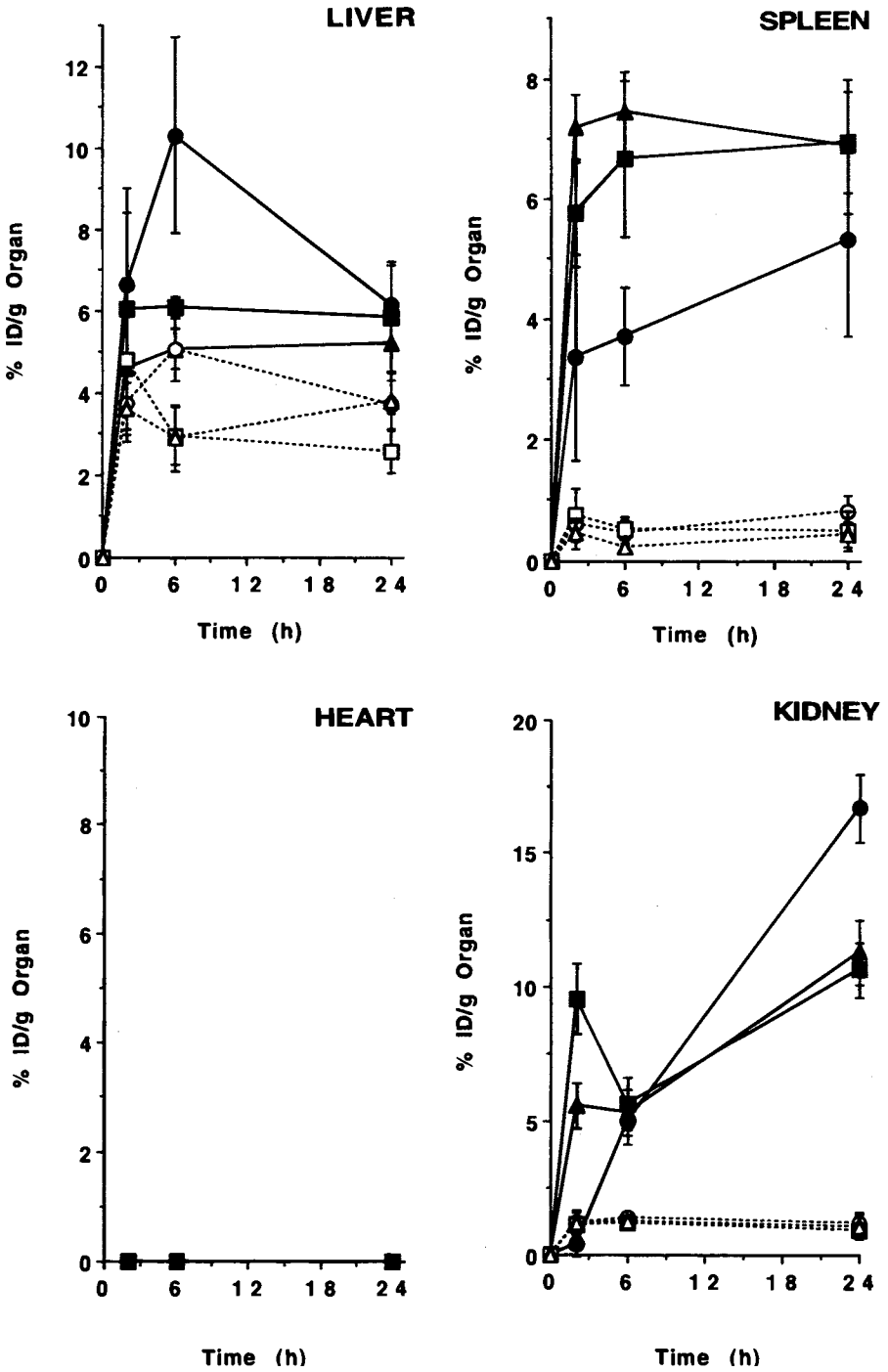

Fig. 2. Organ distribution of DOX and its metabolites in tumor-free organs. Mice with lung metastases (Stage II) were injected with D-SSL and D-SSIL (35 μg DOX/mouse). DOX (solid lines and closed symbols) and total DOX-M (dashed lines and open symbols) were measured at 2, 6, and 24 h post iv injection of D-SSL (●,○), D-SSIL-IgG (■,□) and D-SSIL-32/2 (▲,△). Results are given as percentage of ID per gram organ, corrected for plasma volume (14). The following organ weights were measured (in grams, mean ± S.D.) of: liver (1.01 ± 0.2), spleen (0.11 ± 0.03), both kidneys (0.27 ± 0.03), heart (0.1 ± 0.01), and lungs (0.14 ± 0.2). Statistical analysis (p values). For DOX: *Liver,* D-SSL vs. D-SSIL-IgG and D-SSIL-32/2 < 0.05 at 6 h, > 0.05 at 2 h and 24 h; D-SSIL-32/2 vs. D-SSIL-IgG < 0.05 at 6 h, > 0.05 at 2 h and 24 h. *Spleen,* D-SSL vs. D-SSIL-IgG and D-SSIL-32/2 < 0.005 at 2 h and 6 h, > 0.05 at 24 h; D-SSIL-32/2 vs. D-SSIL-IgG 0.02 at 2 h, > 0.05 at 6 h and 24 h. *Kidney,* D-SSL vs. D-SSIL-IgG and D-SSIL-32/2 < 0.001 at 2 h and 24 h, > 0.05 at 6 h; D-SSIL-32/2 vs. D-SSIL-IgG < 0.001 at 2 h, > 0.05 at 6 h and 24 h. For DOX-M: *Liver,* D-SSL vs. D-SSIL-IgG and D-SSIL-32/2 < 0.05 at 6 h, > 0.05 at 2 h and 24 h; D-SSIL-32/2 vs. D-SSIL-IgG > 0.05 at all time points. *Spleen,* D-SSL vs. D-SSIL-IgG and D-SSIL-32/2 > 0.05 at all time points. *Kidney,* D-SSL vs. D-SSIL-IgG and D-SSIL-32/2 > 0.05 at all time points.

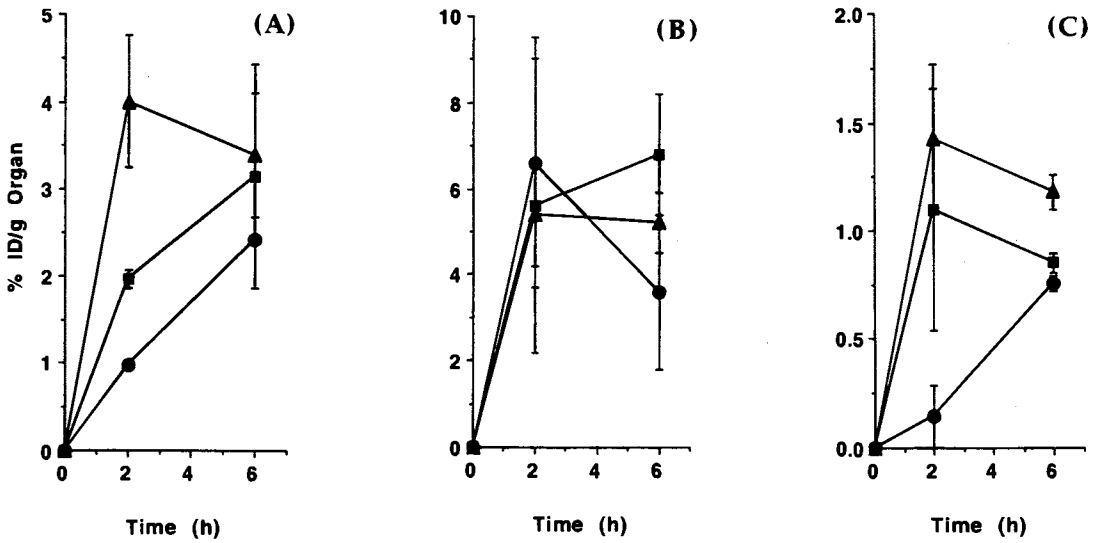

Fig. 3. DOX levels in cancerous lungs at three stages of tumor development after injection of D-SSL or D-SSIL. Mice bearing A9 tumor at Stage I (A), Stage II (B), and Stage III (C) were injected iv with D-SSL (●), D-SSIL-IgG (■), or D-SSIL-32/2 (▲) (35 μg DOX/mouse), and DOX concentration was measured after 2 and 6 h. Results are given as percentage of ID per gram, corrected for plasma content in normal lungs (14). Statistical analysis (p values). Stage I tumor (A): D-SSL vs. D-SSIL-IgG and D-SSIL-32/2 < 0.002 at 2 h, > 0.05 at 6 h; D-SSIL-32/2 vs. D-SSIL-IgG 0.01 at 2 h, > 0.05 at 6 h. Stage II tumor (B): D-SSL vs. D-SSIL-IgG > 0.05 at 2 h, < 0.05 at 6 h, vs. D-SSIL-32/2 > 0.05 at 2 h and 6 h; D-SSIL-32/2 vs. D-SSIL-IgG > 0.05 at 2 h and 6 h. Stage III tumor (C): D-SSL vs. D-SSIL-IgG > 0.05 at 2 h, < 0.05 at 6 h, vs. D-SSIL-32/2 < 0.05 at 2 h, > 0.05 at 6 h; D-SSIL-32/2 vs. D-SSIL-IgG > 0.05 at 2 h, < 0.05 at 6 h.

performance, and (b) determining drug (DOX) metabolism in noncancerous and cancerous tissues of mice injected with the various liposomal preparations. Most of the drug delivered via D-SSL and D-SSIL was present in the plasma, and as intraliposomal drug. Plasma to liver total drug ratios were ~6 (at 2 h post-injection) for both SSL and SSIL. Also, recovery of drug and its metabolites, in plasma plus organs tested, at 6 h post-injection of D-SSL reached 79% of ID (73% for drug and 6% for metabolites). Since not all tissues were evaluated (e.g., the skin), it seems probable that 6 h post-injection all DOX injected as SSL can be accounted for in the mouse body. For DOX delivered via D-SSIL recovery of DOX + DOX-M in all organs tested was about 50% of that determined for D-SSL. The fate of the unrecovered drug for the D-SSIL delivery is not yet clear.

Drug delivered via D-SSIL had a much longer MRT and slower clearance than D-Lip or free DOX (9, and Table 1), although a shorter MRT, faster clearance, and smaller AUC

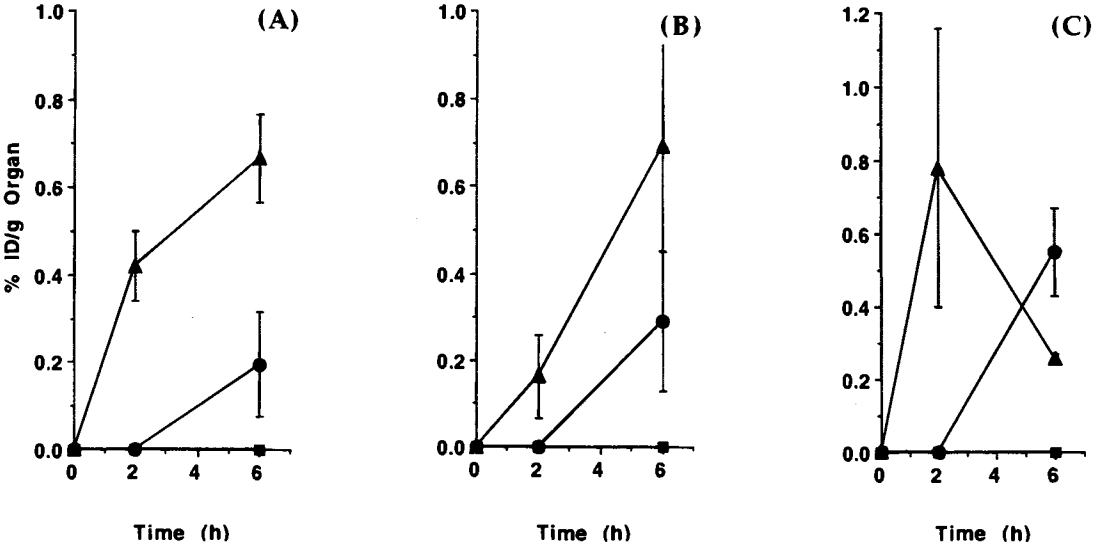

Fig. 4. DOX total metabolite levels in cancerous lungs at different tumor stages in mice injected with D-SSL, D-SSIL-IgG, or D-SSIL-32/2. No metabolites could be detected in mice given D-SSIL-IgG. For more details see legends to Figs. 1 and 3. Statistical analysis (p values). D-SSIL-32/2 vs. D-SSL at 6 h: For Stage I tumor (A) < 0.01, for Stage II tumor (B) < 0.05, for Stage III tumor (C) < 0.05.

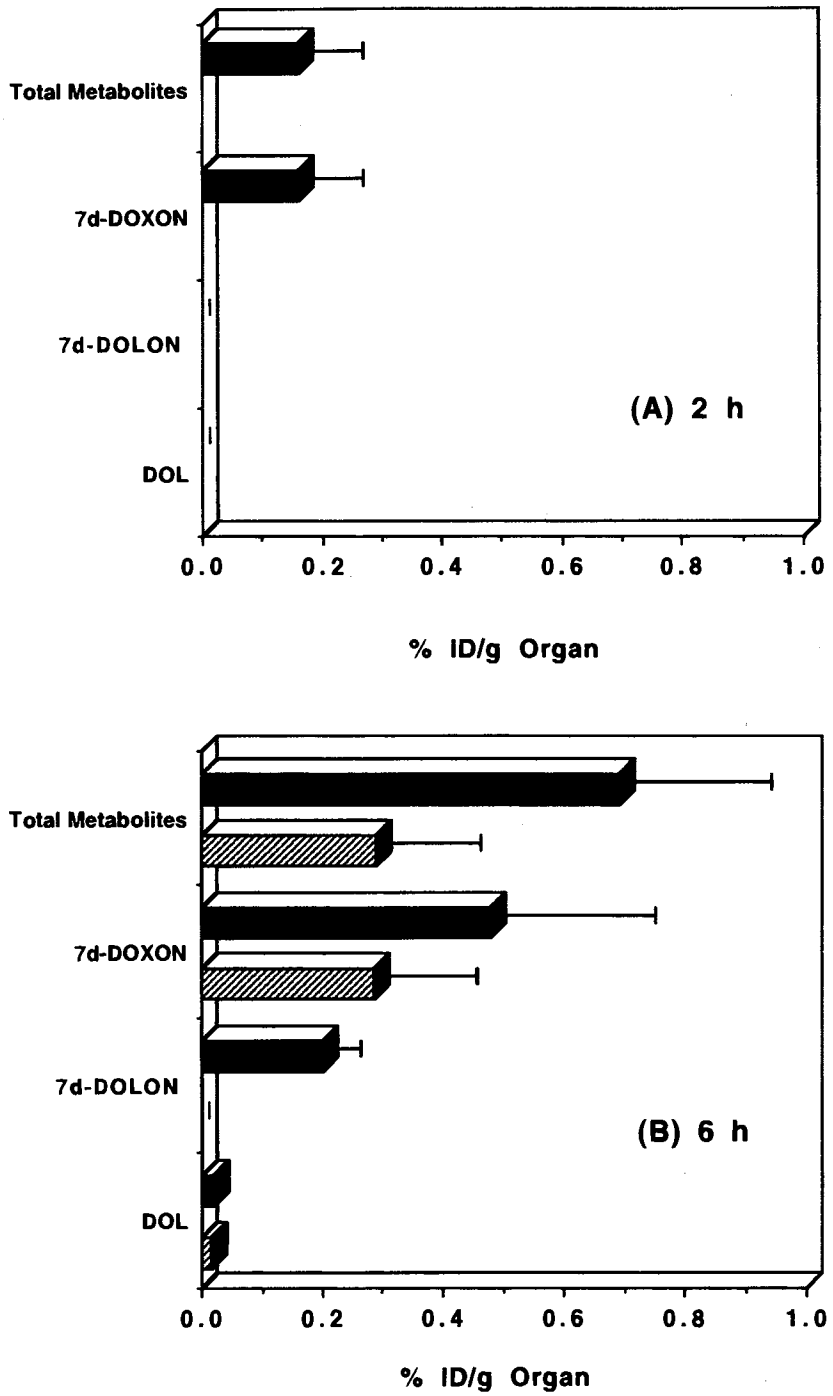

Fig. 5. Quantitative analysis of DOX metabolites in cancerous lungs of mice bearing A9 tumor (Stage II) injected with D-SSIL-32/2, D-SSIL-IgG, or D-SSL (35 μg DOX/mouse). DOX-M were measured 2 h (A) and 6 h (B) after injection. Black bars—D-SSIL-32/2, striped bars—D-SSL. For abbreviations of metabolites, see Materials and Methods.

(Table 1) than DOX delivered via D-SSL. This effect was independent of antibody specificity. The organ biodistribution of DOX and DOX-M, the plasma pharmacokinetics, and the organ biodistribution of D-SSIL and FITC-labeled SSIL, described here and the in vitro data described before (9), suggest that the faster clearance of DOX delivered via D-SSIL, as compared with D-SSL, is due mainly to faster clearance of intact liposomes.

Analysis of DOX levels in non-cancerous organs reveals more similarities than differences between the three liposome preparations in mice carrying tumors of Stage II (Fig. 2) and Stage I (data not shown). This shows that, except for the spleen,

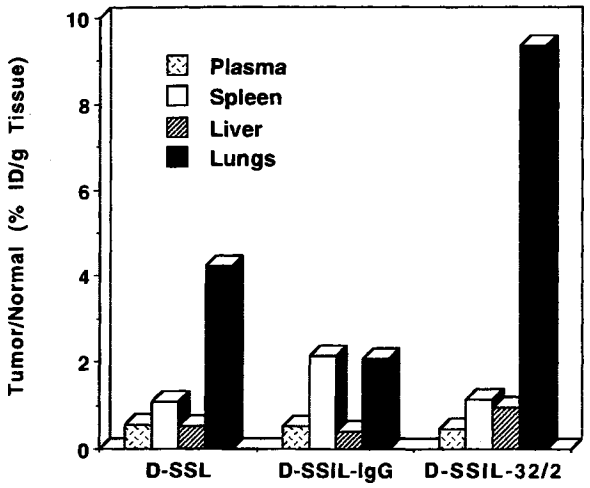

Fig. 6. Selectivity of delivering total drug (DOX + its metabolites) into plasma and organs of tumor-bearing mice. Mice with lung metastases (Stage II) were injected with various liposomal preparations (see text). The selectivity was determined as the ratio of total drug level in tissues of tumor-bearing mice to that in normal mice 24 h after liposome administration.

antibodies present on the D-SSIL surface do not increase drug accumulation in liver or kidney and, more importantly, in heart—the organ most sensitive to DOX toxicity. Therefore, regarding cardiotoxicity, D-SSIL should be equivalent to D-SSL.

Analysis of the pattern of DOX-M in tumor-free organs indicates that there are no qualitative differences and only small quantitative differences between the three preparations, and therefore it can be assumed that the metabolic fate of the drug is similar for all three. The high level of metabolites in the liver indicates that the drug encapsulated in all three vesicle preparations became available.

The major advantage of small (diameter < 120 nm) D-SSL is their ability to extravasate into tumors (1,15). However, their accumulation in the tumor is slow (1,2). The present study shows clearly that DOX accumulation from both D-SSL and D-SSIL is dependent on the tumor stage (Fig. 3). For micrometastases, the presence of the specific MAb on the D-SSIL accelerates DOX accumulation at the tumor site. For specific anti-tumor MAb it is well established that depth and extent of antibody penetration depend on both its size and its affinity to the targeted antigen; the smaller the antibody molecule and the lower the affinity, the deeper and greater is the penetration (16,17). The above, together with the high tumor interstitium pressure (18), is a major obstacle to successful antibody-based therapy for solid tumors. D-SSIL are much larger than the antibodies used for the above comparison (~100 nm vs. 6–12 nm). Moreover, being polyvalent (~15 antibody molecules per vesicle (9,11)), D-SSIL avidity may be higher than the affinity of a single IgG molecule. This may explain our observation (data not shown) that the extravasation has a limited depth of about three layers of tumor cells beyond the endothelium of the tumor blood vessels. It seems that the first D-SSIL-32/2 which attach to their target cells block the penetration of additional D-SSIL-32/2 to deeper layers of the tumor. The fact that in all 3 stages of tumor development tested, accumulation of DOX delivered via D-SSIL-32/2 was practically stopped 2 h post-injection (Fig. 3), in contrast to D-SSL and D-SSIL-IgG, supports the assumption of a blocking effect caused by specific binding to the tumor cells. At the micrometastases stage the tumor is more exposed to the vasculature and, therefore, a larger fraction of the tumor cells is accessible to the immunoliposomes. The D-SSIL-32/2 bind to the target and therefore the level of drug 2 h post-injection is 2–4 times higher than drug delivered via D-SSL. This agrees well with the data of Allen and coworkers, demonstrating the superior antitumor effect in mice of specific D-SSIL, compared to D-SSL, 3 days after tumor inoculation (10). The blocking effect caused by specific interaction with tumor cells may be of special importance at the middle stage of tumor development, since the ratio of zones of low pressure to zones of high pressure is much less favorable than in the micrometastases stage. At Stage III, the necrosis forms regions of low pressure inside the tumor which, theoretically, can allow nonspecific accumulation of all three types of vesicles used in this study. D-SSIL (either specific or nonspecific), due to the nonspecific interaction of most antibodies with various extracellular matrix proteins, including collagen and fibronectin (19), in the necrotic area create a nonspecific blocking effect. Alternatively, this nonspecific binding prevents DOX uptake by the tumor cells since either there is no drug release from the vesicles or the release is too remote from these cells. This may explain the very low ratio of DOX-M/DOX in the cancerous lungs for D-SSIL-IgG treatment described below.

As DOX is metabolized only intracellularly (20), we measured the level of metabolites in the tumor as an indication of drug availability to cells in the cancerous tissue. Differences in DOX-M concentrations between the three liposomal preparations were the most striking results (Figs. 4–6). Drug delivered via D-SSIL-IgG metabolized to a very small extent, in agreement with the lower availability to the tumor cells (see above), while drug delivered by the specific D-SSIL-32/2 gave the highest level of metabolites. It is not yet clear if this difference is related to the way the DOX is taken up by the cells.

To sum up, our study demonstrates that the level of DOX in the tumor, and more so, of its metabolites, is determined by the combined effects of the presence of the targeting antibodies and the exact state of the solid tumor. Experiments underway in our laboratories are aimed at testing the immunogenicity of SSIL as well as the relationship between the pharmacokinetic and biodistribution performance and therapeutic efficacy.

ACKNOWLEDGMENTS

We would like to thank SEQUUS Pharmaceuticals Inc., Menlo Park, CA for the generous gift of ^{2000}PEG-DSPE; Lipoid (Ludwigshafen, Germany) for a gift of HPE; Professor I. Witz, Tel Aviv University, for the A9 tumor cells; Dr. R. Cohen and Dr. M. Brickman of our group for their help with the HPLC; and Mr. S. Geller and Mrs. B. Levene, respectively, for editing and typing the manuscript.

REFERENCES

1. D. Lasic and F. Martin, eds., *Stealth Liposomes.* CRC Press, Boca Raton, Florida, 1995.
2. A. Gabizon, R. Catane, B. Uziely, B. Kaufman, T. Safra, R. Cohen, F. Martin, A. Huang, and Y. Barenholz. Prolonged circulation time and enhanced accumulation in malignant exudates of doxorubicin encapsulated in polyethylene-glycol coated liposomes. *Cancer Res.* **54**:987–992 (1994).
3. P. A. H. M. Toonen and D. J. A. Crommelin. Immunoglobulins as targeting agents for liposome encapsulated drugs. *Pham. Weekbl. Sci.* **5**:269–280 (1983).
4. J. T. P. Derksen, H. W. M. Morselt, and G. L. Scherphof. Uptake and processing of immunoglobulin-coated liposomes by subpopulations of rat liver macrophages. *Biochim. Biophys. Acta* **971**:127–136 (1988).
5. E. Kedar, Y. Rutkowski, E. Braun, N. Emanuel, and Y. Barenholz. Delivery of cytokines by liposomes. 1. Preparation and characterization of interleukin-2 encapsulated in long-circulating sterically stabilized liposomes. *J. Immunother.* **16**:47–59 (1994).
6. A. L. Klibanov, B. A. Khaw, N. Nossiff, S. M. O'Donnell, L. Huang, M. A. Slinkin, and V. P. Torchilin. Targeting of macromolecular carriers and liposomes by antibodies to myosin heavy chain. *Am. J. Physiol.* **261**:60–65 (1991).
7. G. Blume, G. Cevc, D. J. A. Crommelin, I. A. Bakker-Woudenberg, C. Kluft, and G. Storm. Specific targeting with poly(ethylene glycol)-modified liposomes: Coupling of homing devices to the ends of the polymeric chains combines effective target binding with long circulation times. *Biochim. Biophys. Acta* **1149**:180–184 (1993).
8. K. Maruyama, T. Takizawa, T. Yuda, S. J. Kennel, L. Huang, and M. Iwatsuru. Targetability of novel immunoliposomes modified with amphipathic poly(ethylene glycol)s conjugated at their distal terminals to monoclonal antibodies. *Biochim. Biophys. Acta* **1234**:74–80 (1995).
9. N. Emanuel, E. Kedar, E. M. Bolotin, N. I. Smorodinsky, and Y. Barenholz. Preparation and characterization of doxorubicin-loaded sterically stabilized immunoliposomes. *Pharm. Res.* **13**:352–359 (1996).
10. I. Ahmad, M. Longenecker, J. Samuel, and T. M. Allen. Antibody-targeted delivery of doxorubicin entrapped in sterically stabilized liposomes can eradicate lung cancer in mice. *Cancer Res.* **53**:1484–1488 (1993).
11. N. Emanuel, E. Kedar, O. Toker, E. Bolotin, and Y. Barenholz. Steric stabilization of liposomes improves their use in diagnostics. *In:* Lasic, D. D. and Barenholz, Y., eds., *Handbook of Nonmedical Applications of Liposomes,* Vol. IV, CRC Press, Boca Raton, FL, 1996, pp. 229–243.
12. E. M. Bolotin, R. Cohen, L. K. Bar, N. Emanuel, S. Ninio, D. D. Lasic, and Y. Barenholz. Ammonium sulfate gradients for efficient and stable remote loading of amphipathic weak bases into liposomes and ligandoliposomes. *J. Liposome Res.* **4**:455–479 (1994).
13. J. Cummings and C. S. McArdle. Studies on the *in vivo* disposition of adriamycin in human tumours which exhibit different responses to the drug. *Br. J. Cancer* **53**:835–838 (1986).
14. L. Wish, J. Furth, and R. H. Storey. Direct determination of plasma, cell and organ-blood volumes in normal and hyperemic mice. *Proc. Soc. Exp. Biol. Med.* **74**:644–648 (1950).
15. N. Z. Wu, D. Da, T. L. Rudoll, D. Needham, A. R. Whorton, and M. W. Dewhirst. Increased microvascular permeability contributes to preferential accumulation of Stealth liposomes in tumor tissue. *Cancer Res.* **53**:3765–3770 (1993).
16. K. Fujimori, D. G. Covell, J. E. Fletcher, and J. N. Weinstein. Modeling analysis of the global and microscopic distribution of immunoglobulin G, $F(ab')_2$, and Fab in tumors. *Cancer Res.* **49**:5656–5663 (1989).
17. W. van Osdol, K. Fujimori, and J. N. Weinstein. An analysis of monoclonal antibody distribution in microscopic tumor nodules: Consequences of a "binding site barrier". *Cancer Res.* **51**:4776–4784 (1991).
18. R. K. Jain. Physiological resistance to the treatment of solid tumors, *In:* Beverly, A. T., ed., *Drug Resistance in Oncology,* Marcel Dekker, New York, 1993, pp. 87–105.
19. A. A. Rostagno, B. Frangione, and L. Gold. Biochemical studies on the interaction of fibronectin with Ig. *J. Immunol.* **146**:2687–2693 (1991).
20. C. E. Riggs, Jr. and N. R. Bachur. Clinical pharmacokinetics of anthracycline antibiotics. *In:* Ames, M. M., Powis, G., and Kovach, J. S., eds., *Pharmacokinetics of Anticancer Agents in Humans,* Elsevier, Amsterdam, 1983, pp. 229–278.